AGU PUBLICATIONS

JGR

Journal of Geophysical Research: Space Physics

RESEARCH ARTICLE

10.1002/2014JA019964

Key Points:

- Broad plasma depletions (BPDs) are the bottomside phenomena
- BPDs are not associated with the evolution of plasma bubbles
- Ionospheric uplift is responsible for the satellite detection of BPDs

Correspondence to:
H. Kil,
hyosub.kil@jhuapl.edu

Citation:
Kil, H., Y.-S. Kwak, W. K. Lee, S.-J. Oh, M. Milla, and I. Galkin (2014), Broad plasma depletions detected in the bottomside of the equatorial *F* region: Simultaneous ROCSAT-1 and JULIA observations, *J. Geophys. Res. Space Physics*, *119*, 5978–5984, doi:10.1002/2014JA019964.

Received 13 MAR 2014
Accepted 7 JUL 2014
Accepted article online 9 July 2014
Published online 28 JUL 2014

Broad plasma depletions detected in the bottomside of the equatorial *F* region: Simultaneous ROCSAT-1 and JULIA observations

Hyosub Kil[1], Young-Sil Kwak[2], Woo Kyoung Lee[2], Seung-Jun Oh[3], Marco Milla[4], and Ivan Galkin[5]

[1]The Johns Hopkins University Applied Physics Laboratory, Laurel, Maryland, USA, [2]Korea Astronomy and Space Science Institute, Daejeon, South Korea, [3]Space Environment Laboratory, Seoul, South Korea, [4]Radio Observatorio de Jicamarca, Instituto Geofísico del Perú, Lima, Peru, [5]University of Massachusetts Lowell, Lowell, Massachusetts, USA

Abstract We investigated the association of broad plasma depletions (BPDs) with plasma bubbles and ionospheric uplift in the equatorial *F* region using the coincident satellite and radar observations over Jicamarca in Peru. BPDs were detected by the first Republic of China satellite (ROCSAT-1) on the nights of 21 and 22 December 2002 during the period of moderate geomagnetic activity. The observations of the Jicamarca Unattended Long-term Investigations of the Ionosphere and Atmosphere radar and an ionosonde showed that the *F* peak height was lifted above the ROCSAT-1 altitude (600 km) at the times of the BPD detection. The fraction of NO^+ was substantial at the locations of BPDs. These observations support the association of the BPDs with the ionospheric uplift. However, the absence of large backscatter plumes at the times of the BPD detection indicates that the BPDs were not produced by a single large bubble or a merger of bubbles.

1. Introduction

Various scales of plasma depletions appear along satellite orbits in the equatorial *F* region. Among them, the plasma depletions of the zonal or longitudinal width of a few hundred kilometers are often called "bubbles" [e.g., *Makela*, 2006]. Plasma depletions whose zonal widths are greater than several hundred kilometers occasionally occur, and we call them broad plasma depletions (BPDs). BPDs have been detected by satellites near the magnetic equator in the altitude range of 350–840 km [*Basu et al.*, 2001, 2007; *Burke et al.*, 2000, 2009; *Greenspan et al.*, 1991; *Huang et al.*, 2011, 2012; *Kil and Paxton*, 2006; *Kil and Lee*, 2013; *Kil et al.*, 2006; *Lee et al.*, 2014; *Su et al.*, 2002]. The BPD phenomenon has been considered to be associated with geomagnetic storms because most studies reported the BPDs observed during magnetically disturbed periods. However, BPDs also occur during magnetically quiet periods when the satellite altitude is low (~400 km) [*Lee et al.*, 2014].

The hypotheses regarding the source of BPDs are divided largely into two categories. One category explains the BPD phenomenon in terms of the relative altitudes of satellites and *F* region [*Basu et al.*, 2001, 2007; *Greenspan et al.*, 1991; *Kil and Lee*, 2013; *Lee et al.*, 2014; *Su et al.*, 2002]. According to this hypothesis, the occurrence of BPDs along a satellite orbit is related to the sampling of the ionosphere in the bottomside of the *F* region. BPDs may occur more frequently during magnetically disturbed periods than during magnetically quiet periods because the ionosphere is lifted to high altitudes by storm-induced electric fields [e.g., *Basu et al.*, 2007]. In the other hypothesis category, bubbles are considered the source of BPDs; BPDs are produced by a development of abnormally large bubbles during geomagnetic storms [*Burke et al.*, 2000, 2009] or by a merger of regular bubbles [*Huang et al.*, 2011, 2012; *Kil and Paxton*, 2006; *Kil et al.*, 2006]. The bubble-related hypotheses arose from the observations of bubbles coincidently with BPDs. The first hypothesis category views BPDs as bottomside phenomena, whereas the second hypothesis category views BPDs as topside phenomena.

We report the BPD events that support the former hypothesis (association of BPDs with ionospheric uplift). We have searched for BPDs that occur near the Jicamarca Radio Observatory (JRO) (11.95°S, 76.87°W) using the first Republic of China satellite (ROCSAT-1) (later renamed as FORMOSAT-1) data. ROCSAT-1 was launched on 27 January 1999 to a circular orbit at an altitude of 600 km. Its orbital inclination was 35°. The ROCSAT-1 mission was ended on 17 June 2004. This study uses the measurements of the ion density and

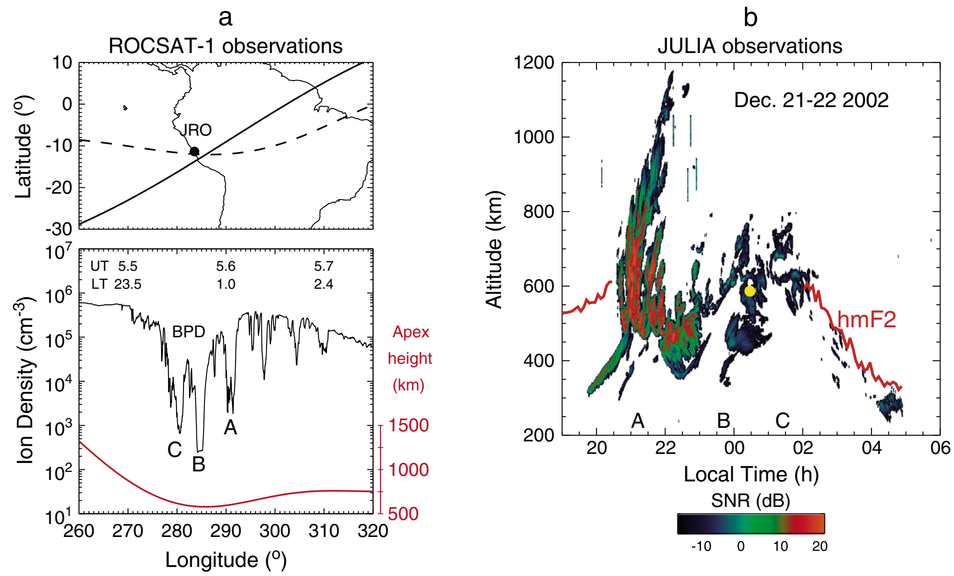

Figure 1. ROCSAT-1 and JULIA observations on 21 and 22 December 2002. (a) ROCSAT-1 orbit and measurements of plasma density along the ROCSAT-1 orbit. The magnetic equator is shown by a dashed line. The red curve is the magnetic apex height of the ROCSAT-1 orbit. (b) JULIA backscatter power map. The red curve shows the *F* peak height (h_mF_2) derived from ionosonde observations. The magnetic apex height of the ROCSAT-1 orbit at the time of its pass over JRO is shown by a yellow dot.

velocity by the Ionospheric Plasma and Electrodynamics Instrument on board ROCSAT-1 [*Yeh et al*., 1999]. Among the BPDs identified during the period of March 1999 to June 2004, we present two events detected on the nights of 21 and 22 December 2002. The Jicamarca Unattended Long-term Investigations of the Ionosphere and Atmosphere (JULIA) radar observations were available on those nights. JULIA is a 50 MHz coherent backscatter radar that has been operated since August 1996 [*Hysell and Burcham*, 1998]. Moderate level of geomagnetic activity (average disturbance storm time (*Dst*) index = −38 nT) persisted during 20–24 December 2002. The planetary *k* (*Kp*) indices at the times of the BPD detection on the nights of 21st and 22nd were 1^+ and 3^0, respectively.

2. Results and Discussion

JULIA observations are used to identify the existence of bubbles at the locations of BPDs and the ionospheric conditions at the times of the BPD detection. Bubbles appear as vertical backscatter plumes in radar observations. If BPDs are associated with bubbles (either a single large bubble or a merger of bubbles), large plumes are expected to appear at the locations of BPDs. If the ionospheric uplift is responsible for BPDs, the satellite altitude at the time of the BPD detection should be in the bottomside *F* region. The ionosonde observations of the *F* peak height (h_mF_2) provide an additional tool for identifying the existence of the ionospheric uplift.

The ROCSAT-1 orbit and the 1 s average plasma density on 21 and 22 December 2002 are shown in Figure 1a. The red curve is the projection altitude of the ROCSAT-1 orbit onto the magnetic equator along the magnetic field lines (magnetic apex height). On that night, plasma depletions appear in broad longitude range over South America. Three depletions are indicated by letters "A," "B," and "C" to compare with the JULIA observations in Figure 1b. Depletions B and C appear under a trough-like depletion which we call a BPD. In the JULIA signal-to-noise ratio map, the magnetic apex height of the ROCSAT-1 orbit at the time of the ROCSAT-1 pass over JRO is shown by a yellow dot. The red line is the h_mF_2 derived from the ionosonde observations at JRO.

A large backscatter plume appears near 21 local time (LT). This plume is not related to the BPD because the plume appeared a few hours before the detection of the BPD. Considering the eastward motion of the ionosphere at night, the depletion associated with the plume is likely Depletion A. We can identify this by

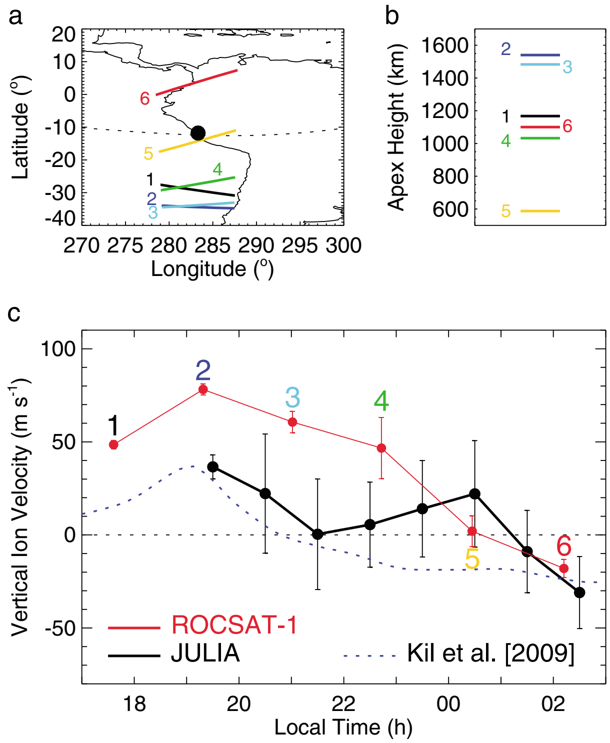

Figure 2. Vertical ionospheric motions observed by ROCSAT-1 and JULIA on 21 and 22 December 2002. (a) ROCSAT-1 orbits. (b) Magnetic apex heights of ROCSAT-1 orbits. (c) Average vertical velocities. Red dots represent the average velocities along the ROCSAT-1 orbits shown in Figure 2a. Blue dots represent the average velocities obtained from the JULIA data at an altitude range of 300–700 km. The vertical drift in December in the Perubian sector derived from empirical model [*Kil et al.*, 2009] is shown with a blue dotted line.

using the measurements of the zonal plasma velocity. The average eastward plasma drift velocities between 2.0 (the detection time of the plume by JULIA) and 5.6 (the detection time of Depletion A by ROCSAT-1) universal time (UT) calculated with the JULIA and ROCSAT-1 data are 79 and 118 m s^{-1}, respectively. The JULIA velocity is the average velocity in the altitude range of 300–700 km. If the large plume detected at 21 LT (02 UT) drifted eastward with the velocity of 79 m s^{-1} for 3.6 h, the plume would be found near 291°E. Depletion A is exactly at 291°E. With the velocity (118 m s^{-1}) derived from ROCSAT-1, the plume is predicted to be found near 296°E. We interpret that the velocity observed by JULIA properly represents the plasma motion at the magnetic equator. If the depletions observed at 294°–300°E were associated with the large plume, a similar large plume is expected to appear around 22–23 LT to account for Depletion A. However, only small plume features appear at that time. The approximate passing times of depletions A, B, and C are indicated in Figure 1b with the corresponding letters. The backscatter layer below vertical plumes can be considered to be produced by turbulence in the bottomside. Extension of the h_mF_2 following the backscatter layer at 02–05 LT reaches above an altitude of 600 km at 01 LT. The ROCSAT-1 orbit (yellow dot) is below this height. Thus, the trough-like depletion (or BPD) in Figure 1a is associated with the ROCSAT-1 orbit in the bottomside. The absence of large plumes at the times of the BPD detection indicates that the creation of the BPD is not associated with a development of an abnormally large bubble or a merger of bubbles.

We further investigate the vertical motion of the ionosphere using the ROCSAT-1 and JULIA observations. The six consecutive ROCSAT-1 orbits on 21 and 22 December are shown in Figure 2a, and the average magnetic apex heights of those orbits are shown in Figure 2b. The ROCSAT-1 orbit in Figure 1a corresponds to Orbit 5 in Figure 2a. Except for Orbit 5, the magnetic apex heights of all orbits are above 1000 km. The average vertical velocities calculated using the data along the ROCSAT-1 orbits in Figure 2a are shown with red dots in Figure 2c. The average vertical velocities derived from JULIA observations at an altitude range of 300–700 km are shown with black dots. The vertical bars are the standard deviations. As a reference, the vertical ion velocity over JRO in December obtained from the empirical model [*Kil et al.*, 2009] is shown with a blue dotted line. The empirical model was derived from ROCSAT-1 observations under a magnetically quiet condition, and the model presented in Figure 2c represents the vertical ion velocity during a solar maximum (the solar flux index $F_{10.7} > 180$ (10^{-22} W m^{-2} Hz^{-1})). Both the ROCSAT-1 and JULIA observations show that the vertical drift of the ionosphere was significant on the night of the 21st compared with the climatological drift pattern. In the ROCSAT-1 observation, the average vertical velocity between 21 and 23 LT (velocities at the points 3 and 4 in Figure 2c) is 54 m s^{-1}. With this velocity, the *F* region is lifted 389 km for 2 h. This means that the *F* peak height reaches near 1000 km at 23 LT. However, this scenario is unrealistic considering the morphology of the backscatter echoes and ionosonde observations. On the other hand, the drift pattern derived from the JULIA observation agrees with the morphology of the backscatter echoes and ionosonde observations. Because the

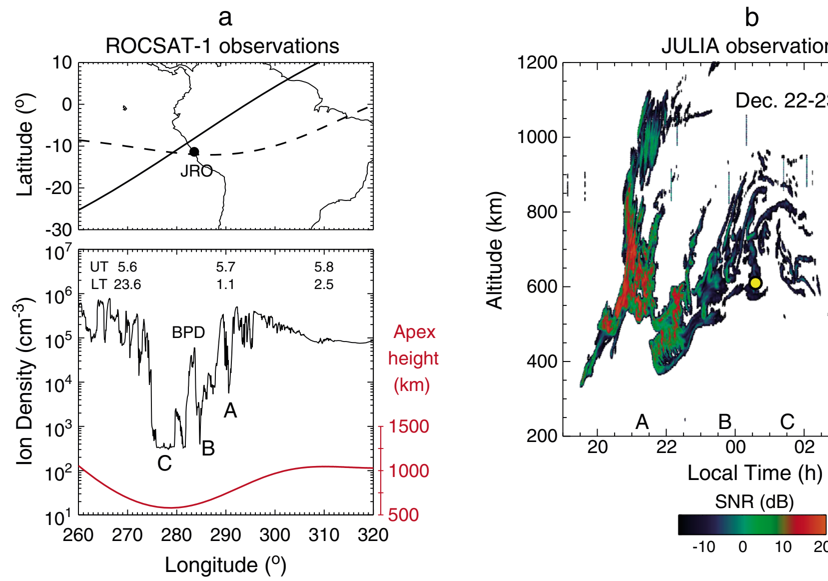

Figure 3. ROCSAT-1 and JULIA observations on 22 and 23 December 2002. The format is the same as Figure 1.

plasma motion can vary with altitude and latitude, the JULIA observations may better represent the plasma motions at the magnetic equator in the altitude region of our interest.

More convincing evidence of the uplift of the bottomside to the ROCSAT-1 altitude is provided by the observations on the following day. Figure 3 is the same format as Figure 1 for the observations on 22–23 December 2002. The occurrence times of bubbles and the morphology of the backscatter echoes in Figure 3 are similar to those in Figure 1. If the zonal drift of the ionosphere on the night of the 22nd were similar to that on the night of the 21st, Depletion A would correspond to the large backscatter plume observed near 21 LT. The average eastward velocity between 2.0 (the detection time of the large plume by JULIA) and 5.7 (the detection time of Depletion A by ROCSAT-1) UT was 71 m s^{-1} in both the ROCSAT-1 and JULIA observations. This velocity is close to the velocity observed by JULIA on the night of 21st. With the velocity of 71 m s^{-1}, the depletion associated with the large plume is predicted to drift about 7.8° in longitude between 2.0 and 5.7 UT. Depletion A is exactly at the predicted longitude (291°E).

We note two differences between observations in Figures 1 and 3. Depletions B and C in Figure 3a are broader than those in Figure 1a. The individual Depletions B and C in Figure 3a may be called BPDs. The other difference is the height of the backscatter layer. On average, the height of the backscatter layer in Figure 3b is higher

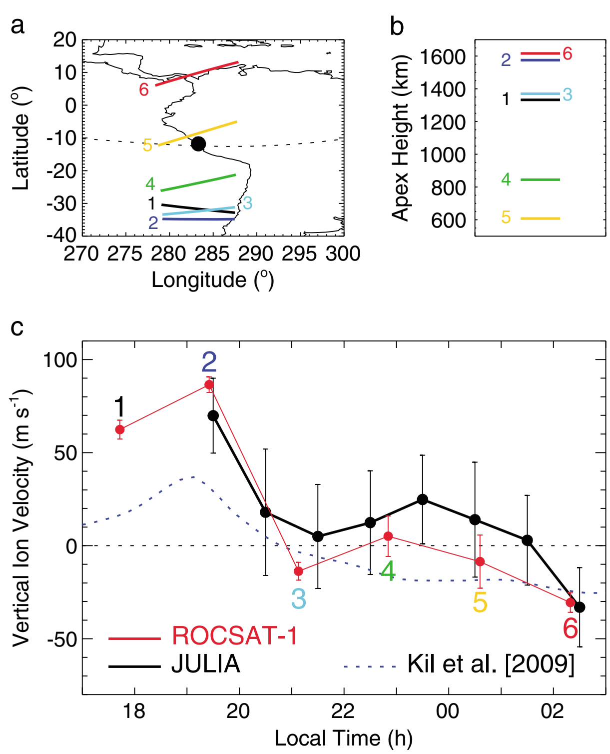

Figure 4. Vertical ionospheric motions observed by ROCSAT-1 and JULIA on 22 and 23 December 2002. The format is the same as Figure 2.

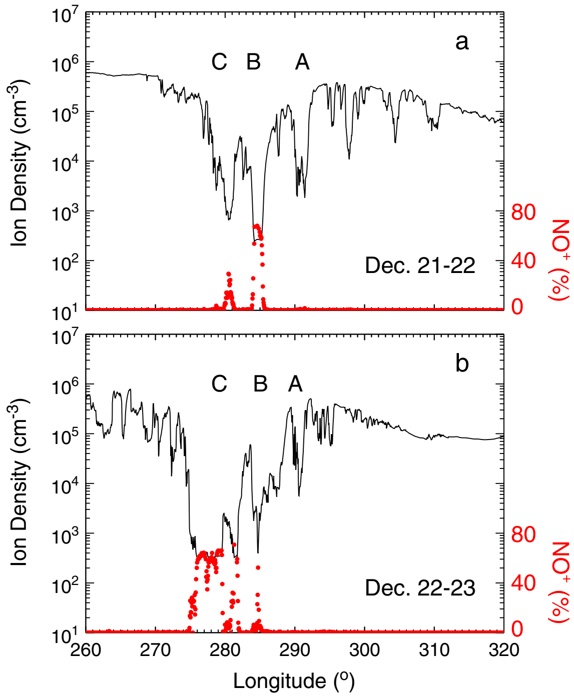

Figure 5. ROCSAT-1 observations of plasma density (black curves) and NO^+ fraction (red dots) on (a) 21 and 22 and (b) 22 and 23 December 2002.

by about 50–100 km compared with that in Figure 1b. The thin backscatter layer after 0200 LT in Figure 3b is similar to that observed in Figure 1b and is considered to be located just below h_mF_2 (ionosonde observations were not available on the night of the 22nd). This layer reaches near 700 km, about 100 km higher than the ROCSAT-1 orbit, at the time of the BPD detection. On the basis of the morphology of the backscatter echoes, the uplift of the ionosphere was more significant on the night of 22nd than on the night of 21st. The detection of broader depletions on the night of 22nd is attributed to the difference of the ionospheric uplift on two nights.

Figure 4 is the same format as Figure 2 for the ROCSAT-1 and JULIA observations on the 22nd and 23rd. Both the ROCSAT-1 and the JULIA observations demonstrate the existence of a significant ionospheric uplift before 21 LT. The uplift persists until 01 LT in the JULIA observation, but it is minor in the ROCSAT-1 observation. Considering the morphology of the backscatter echoes that shows the rise of the bottomside backscatter layer until 01 LT, the drift pattern observed by JULIA better represents the vertical motion of the equatorial ionosphere on that night. If we compare the vertical drifts observed by JULIA in Figures 2c and 4c, the uplift was more significant on the night of 22nd than on the night of 21st, and these observations are consistent with the difference of the heights of the backscatter echoes on those nights.

Because the fraction of molecular ions in the total ion density increases with the decrease of altitude in the bottomside, it can be used as an indicator of the severity of the ionospheric uplift [e.g., *Su et al.*, 2002]. Figure 5 shows the ROCSAT-1 observations of the NO^+ fraction and plasma density on (a) 21 and 22 and (b) 22 and 23 December 2002. The NO^+ fraction is substantial at the locations of Depletions B and C on both days. On both nights, NO^+ is detected at the depletions whose densities are ~10^3 cm^{-3}. The substantial NO^+ fraction and low plasma density at Depletions B and C indicate that those depletions originate from the lower parts of the bottomside than other depletions do. As can be seen from Figures 2b and 3b, Depletions B and C occur when the bottomside is lifted to the altitude of ROCSAT-1. If bubbles develop under that condition, ROCSAT-1 detects lower plasma density and higher NO^+ fraction at those bubbles than at the bubbles that develop when the *F* region is not lifted. Depletions B and C on both nights are explained by the combined effect of the ionospheric uplift and creation of bubbles.

The width and depth of BPDs detected along a satellite pass depend on the severity of the ionospheric uplift and the satellite altitude. The presence of bubbles also affects BPD width and depth. For the BPD events reported by *Kil and Lee* [2013], large BPDs were detected because the satellite altitudes were low (<470 km) in addition to the ionospheric uplift. The BPDs detected by ROCSAT-1 may not be as large as the BPDs reported by *Kil and Lee* [2013] because the altitude of ROCSAT-1 was high (~600 km). The BPD in Figure 1b has a trough-like shape whose plasma depletion is less severe compared with that at the BPDs in Figure 3b, although those BPDs were detected at similar altitudes. On the basis of the morphology of the backscatter echoes and the vertical plasma drift observed by JULIA, the difference of the severity of the ionospheric uplift is considered the primary cause of the difference of the BPD morphology on the two nights. The other factor that affects the morphology of a BPD is the existence of bubbles. *Lee et al.* [2014] pointed out that a BPD has either smooth walls or steep walls depending on the presence of bubbles. If multiple and large bubbles developed as a consequence

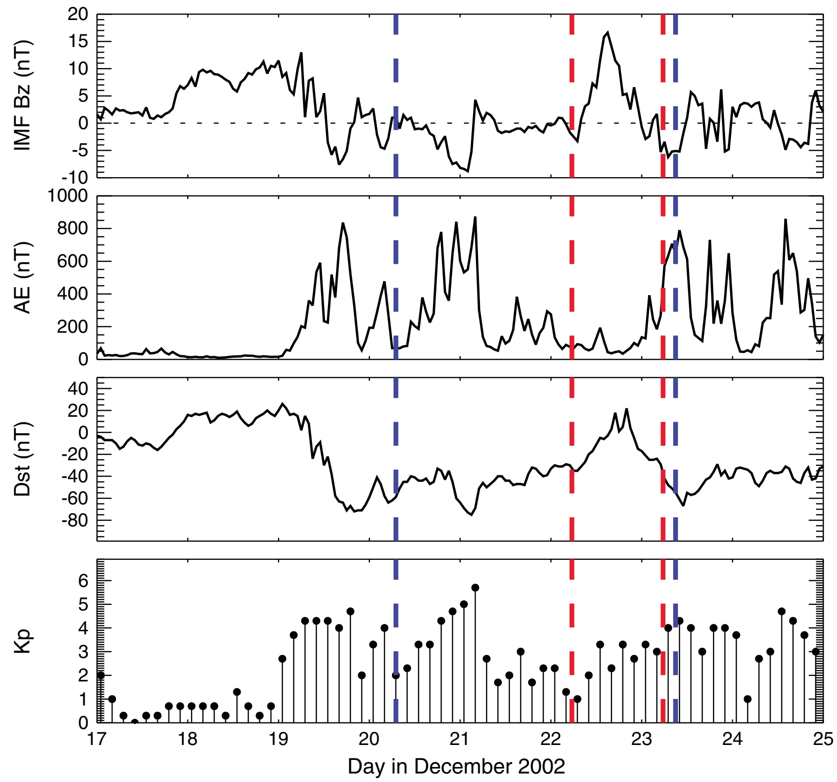

Figure 6. Magnetic indices. (first panel) IMF B_z, (second panel) *AE* index, (third panel) *Dst* index, and (fourth panel) *Kp* index are shown. The red dashed lines indicate the times of the BPD detection over JRO. The blue dashed lines indicate the times of the BPD detection in other longitude regions.

of the uplift of the ionosphere, then a satellite in the bottomside would detect a deeper and wider BPD in that region than in the region where bubbles were absent.

BPDs occasionally occur in the ROCSAT-1 observations. It means that the uplift of the *F* peak height above an altitude of 600 km is unusual. The unusual uplift of the ionosphere on the nights of 21st and 22nd is considered to be associated with storm-induced electric fields. The magnetic indices in December 2002 obtained from the National Aeronautics and Space Administration website (http://omniweb.gsfc.nasa.gov/form/dx1.html) are presented in Figure 6. Figure 6 (first to fourth panels) shows the vertical component of the interplanetary magnetic field (IMF) at 1.54×10^6 km toward the Sun from the Earth center, auroral electroject (*AE*) index, *Dst* index, and *Kp* index. The detection times of BPDs over JRO (the observations presented in this study) are indicated with vertical red lines. The vertical blue lines indicate the times of the BPD detection by ROCSAT-1 in other longitudes. All those BPDs were detected when ROCSAT-1 crossed the magnetic equator. During December 2002 and January 2003, the geomagnetic activity was most pronounced on 19–27 December 2002, and BPDs were detected only in this storm period. Thus, the occurrence of those BPDs is likely associated with storm-induced electric fields. With our data set, we cannot clarify whether the ionospheric uplift was caused by penetration electric fields or disturbance dynamo electric fields.

We note that geomagnetic storms do not warrant the occurrence of BPDs in the ROCSAT-1 observations. In addition to the effect of storm-induced electric fields, quiet time ionospheric dynamics seems to be an important factor for the occurrence of BPDs. In the Peruvian sector, the postsunset vertical motion of the ionosphere is more significant in December than in June [e.g., *Fejer et al.*, 1991]. If the ionospheric uplift occurred at premidnight in that sector by the effect of storm-induced electric fields, a satellite would have a higher chance to detect a BPD in December than in June because the height of the ionosphere is higher in December than in June. The occurrence of the storm in December may contribute to the occurrence of BPDs even during the period of moderate geomagnetic activity.

3. Conclusions

We have investigated the origin of abnormally broad plasma depletions (we call BPDs) in the equatorial *F* region by comparing the coincident satellite (ROCSAT-1) and radar (JULIA) observations on 21 and 22 and 22 and 23 December 2002 over Jicamarca in Peru. In JULIA observations, large plumes do not exist at the times of the BPD detection, and therefore, the BPDs were not produced by a single large bubble or by the merger of bubbles. The radar and ionosonde observations demonstrate the existence of significant uplift of the *F* region on those nights. Because the BPDs were detected during the period of geomagnetic activity, storm-induced electric fields might be responsible for the ionospheric uplift. When ROCSAT-1 detected BPDs, its orbits were in the bottomside. The NO^+ fraction was substantial at the locations of BPDs. These observations provide clear evidence of the association of the BPD phenomenon with the ionospheric uplift.

Acknowledgments
H. Kil acknowledges support from National Science Foundation Aeronomy program (AGS-1237276). Y.-S. Kwak acknowledges support by a grant from the U.S. Air Force Research Laboratory, under agreement FA 2386-14-1-4004 and by the "Study of near-Earth effects by CME/HSS" project from Korea Astronomy and Space Science Institute. The Jicamarca Radio Observatory is a facility of the Instituto Geofísico del Perú operated with support from National Science Foundation Cooperative agreement AGS-0905448 through Cornell University. The JULIA data for this paper are available at the CEDAR Madrigal Database (http://cedar.openmadrigal.org). The ionosonde data at Jicamarca and the ROCSAT-1 data are available by contacting I. Garkin and H. Kil, respectively.

Alan Rodger thanks the reviewers for their assistance in evaluating this paper.

References

Basu, S., et al. (2001), Ionospheric effects of major magnetic storms during the International Space Weather Period of September and October 1999: GPS observations, VHF/UHF scintillations, and in situ density structures at middle and equatorial latitudes, *J. Geophys. Res.*, *106*(A12), 30,389–30,413, doi:10.1029/2001JA001116.

Basu, S., S. Basu, F. J. Rich, K. M. Groves, E. MacKenzie, C. Coker, Y. Sahai, P. R. Fagundes, and F. Becker-Guedes (2007), Response of the equatorial ionosphere at dusk to penetration electric fields during intense magnetic storms, *J. Geophys. Res.*, *112*, A08308, doi:10.1029/2006JA012192.

Burke, W. J., A. G. Rubin, N. C. Maynard, L. C. Gentile, P. J. Sultan, F. J. Rich, O. de La Beaujardière, C. Y. Huang, and G. R. Wilson (2000), Ionospheric disturbances observed by DMSP at middle to low latitudes during the magnetic storm of June 4–6, 1991, *J. Geophys. Res.*, *105*(A8), 18,391–18,405, doi:10.1029/1999JA000188.

Burke, W. J., O. de La Beaujardière, L. C. Gentile, D. E. Hunton, R. F. Pfaff, P. A. Roddy, Y.-J. Su, and G. R. Wilson (2009), C/NOFS observations of plasma density and electric field irregularities at post-midnight local times, *Geophys. Res. Lett.*, *36*, L00C09, doi:10.1029/2009GL038879.

Fejer, B. G., E. R. de Paula, S. A. González, and R. F. Woodman (1991), Average vertical and zonal *F* region plasma drifts over Jicamarca, *J. Geophys. Res.*, *96*, 13,901–13,906, doi:10.1029/91JA01171.

Greenspan, M. E., C. E. Rasmussen, W. J. Burke, and M. A. Abdu (1991), Equatorial density depletions observed at 840 km during the great magnetic storm of March 1989, *J. Geophys. Res.*, *96*(A8), 13,931–13,942, doi:10.1029/91JA01264.

Huang, C.-S., O. de La Beaujardière, P. A. Roddy, D. E. Hunton, R. F. Pfaff, C. E. Valladares, and J. O. Ballenthin (2011), Evolution of equatorial ionospheric plasma bubbles and formation of broad plasma depletions measured by the C/NOFS satellite during deep solar minimum, *J. Geophys. Res.*, *116*, A03309, doi:10.1029/2010JA015982.

Huang, C.-S., J. M. Retterer, O. de La Beaujardière, P. A. Roddy, D. E. Hunton, J. O. Ballenthin, and R. F. Pfaff (2012), Observations and simulations of formation of broad plasma depletions through merging process, *J. Geophys. Res.*, *117*, A02314, doi:10.1029/2011JA017084.

Hysell, D. L., and J. D. Burcham (1998), JULIA radar studies of equatorial spread *F*, *J. Geophys. Res.*, *103*(A12), 29,155–29,16, doi:10.1029/98JA02655.

Kil, H., and W. K. Lee (2013), Are plasma bubbles a prerequisite for the formation of broad plasma depletions in the equatorial *F* region?, *Geophys. Res. Lett.*, *40*, 3491–3495, doi:10.1002/grl.50693.

Kil, H., and L. J. Paxton (2006), Ionospheric disturbances during the magnetic storm of 15 July 2000: Role of the fountain effect and plasma bubbles for the formation of large equatorial plasma density depletions, *J. Geophys. Res.*, *111*, A12311, doi:10.1029/2006JA011742.

Kil, H., L. J. Paxton, S.-Y. Su, Y. Zhang, and H. Yeh (2006), Characteristics of the storm-induced big bubbles (SIBBs), *J. Geophys. Res.*, *111*, A10308, doi:10.1029/2006JA011743.

Kil, H., S.-J. Oh, L. J. Paxton, and T.-W. Fang (2009), High-resolution vertical drift model driven from the ROCSAT-1 data, *J. Geophys. Res.*, *114*, A10314, doi:10.1029/2009JA014324.

Lee, W. K., H. Kil, Y.-S. Kwak, L. J. Paxton, Y. Zhang, I. Galkin, and I. S. Batista (2014), Equatorial broad plasma depletions associated with the enhanced fountain effect, *J. Geophys. Res. Space Physics*, *119*, doi:10.1002/2013JA019137.

Makela, J. J. (2006), A review of imaging low-latitude ionospheric irregularity processes, *J. Atmos. Sol. Terr. Phys.*, *68*, 1441–1458.

Su, S.-Y., H. C. Yeh, C. K. Chao, and R. A. Heelis (2002), Observation of a large density dropout across the magnetic field at 600 km altitude during the 6–7 April 2000 magnetic storm, *J. Geophys. Res.*, *107*(A11), 1404, doi:10.1029/2001JA007552.

Yeh, H. C., S.-Y. Su, R. A. Heelis, and J. M. Wu (1999), The ROCSAT-1 IPEI preliminary results: Vertical ion drift statistics, *Terr. Atmos. Oceanic Sci.*, *10*, 805–820.